

# DFT Investigation of Chelation of Divalent Cations by Some 4-Benzylidenamino-4,5-Dihydro-1H-1,2,4-Triazol-5-One Derivatives

Bikélé Mama Désiré<sup>1\*</sup>, Zobo Mfomo Joseph<sup>2</sup>, Lissouck Daniel<sup>3</sup>, Younang Elie<sup>4</sup>, Nono Jean Hubert<sup>5</sup> and Mbaze Meva'a Luc<sup>1</sup>

1. Department of Chemistry, Faculty of Science, University of Douala, Douala 24157, Cameroun

2. Department of Forestry and Wood Engineering, University of Douala, Advances Teachers Training College for Technical Education, Douala 1872, Cameroon

3. Department of Physic, Faculty of Science, University of Douala, Douala 24157, Cameroon

4. Department of Inorganic Chemistry, Faculty of Science, University of Yaoundé I, Yaoundé 812, Cameroon

5. Department of Chemistry, Faculty of Science, University of Dschang, Dschang 67, Cameroon

**Abstract:** The complexation of BDHTD (4-benzylidenamino-4,5-dihydro-1H-1,2,4-triazol-5-one derivatives) by divalent doubly charged metal ions  $M^{2+}$  ( $M = \text{Mg, Ca, Fe and Cu}$ ) has been investigated using the density functional method B3LYP. Two distinct coordination modes ( $k^2\text{-O}_2\text{O}$  and  $k^2\text{-O}_2\text{N}$ ) have been taken into account. Geometry optimizations have been performed in gas-phase and solution-phase: acetonitrile and DMF (N,N-dimethylformamide) with the basis set 6-31G(d,p). The B3LYP method was also used to calculate the stability and free energies of the 24 complexes of BDHTD with metal ions  $M^{2+}$  ( $M = \text{Mg, Ca, Fe and Cu}$ ) respectively in gas-phase and solution-phase: acetonitrile and DMF. Results indicate that  $k^2\text{-O}_2\text{N}$  structures are most stable in gas-phase. The influence of substitution on the stability is sensitive in solution-phase. The interaction energies of complexation process in various media have been calculated at B3LYP/6-31G(d,p) and CCSD(T) level. The MIA (metal ion affinity) of BDHTD with  $M^{2+}$  ( $M = \text{Mg, Ca, Fe and Cu}$ ) in various media has been explored. The results show that the MIA highly varies with the coordination mode and substitution effect. From the calculated Gibb energies of complexation in various media, it is revealed that the complexation is possible in gas in acetonitrile. The ligand's affinity toward individual cation  $M^{2+}$  ( $M = \text{Mg, Ca, Fe and Cu}$ ) has been analysed. A significant reduce of BDEs observed confirms the decrease of the antioxidant activity by the metal chelation. The charge transfer induced by metal chelation is examined using the NBO analysis.

**Key words:** Metal chelation, BDHTD, MIA, BDEs, ligand's affinity.

## 1. Introduction

The use of thiosemicarbazide has become in organic synthesis a classical strategy of the synthesis for several heterocycles. Among the increasing number of heterocyclic nitrogen containing compounds, which are pursued in both industry and academia, 1,2,4 triazole derivatives are also interesting targets for drugs design. In general, 1,2,4 triazole derivatives are

biologically versatile compounds displaying a variety of biological effects which include anti-inflammatory [1], antimycobacterial [2-3], antifungal [4], antibacterial [5-6] and antiviral activities [3]. The 4-benzylidenamino-4,5-dihydro-1H-1,2,4-triazol-5-one derivatives obtained through the reaction [7] of 3-alkyl(aryl)-4-amino-4,5-dihydro-1H-1,2,4-triazol-5-ones with 3,4 dihydroxy benzaldehyde, possess various biological properties such as anticonvulsant [7], antifungal [8-9], antituberculosis [10] and antiproliferative [11] activities. In addition, 4,5-dihydro-1H-1,2,4-triazol-5-one derivatives which

\*Corresponding author: Bikélé Mama Désiré, Senior Lecturer, research field: theoretical chemistry. E-mail: bikelemama@yahoo.fr.

exhibit important pharmacological activities such as antiviral [12] and antioxidant [13-14] have found wide use in medicinal chemistry as common structures.

Some 4,5-dihydro-1H-1,2,4-triazol-5-one derivatives were titrated potentiometrically against tetrabutylammonium hydroxide in non-aqueous solvent [15]. The determination of pK<sub>a</sub> values of active constituents of certain pharmaceutical preparation is important, because their distribution, transport behaviours, bonding to receptor and contributions to metabolic behaviour depend on ionization constant [16]. Haydar and al [17] have reported the pK<sub>a</sub> values of eight 4-benzylidenamino-4,5-dihydro-1H-1,2,4-triazol-5-one derivatives using potentiometric titration against tetrabutylammonium hydroxide in aqueous solvents and analysed its antioxidant activities which has been focused only on a reverse correlation between DPPH (2,2 diphenyl-1-picrylhydrazyl) radical scavenging activity and structures [16].

The mechanism by which the 4-benzylidenamino-4,5-dihydro-1H-1,2,4-triazol-5-one derivatives carry out the antioxidant activity has not been elucidated yet. Theoretical studies on SAR (structure-activity relationships) of these compounds should complement experimental investigations. However, to the best of our knowledge, no calculation of the antioxidant activity of 4-benzylidenamino-4,5-dihydro-1H-1,2,4-triazol-5-one derivatives has been reported so far. In our previous work done in various non-aqueous solvent, the relative antioxidant activities of 4-benzylidenamino-4,5-dihydro-1H-1,2,4-triazol-5-one derivatives was investigated [18]. It was pointed out that the phenolic moiety has a higher antioxidant activity than the 1,2,4-triazole homolog. It is well known that chelating effect toward TM (transition metal) ions by antioxidant molecules may not activate metal ion and potentially inhibit the metal-dependent processes [19]. Free iron(II) ions catalyze the production of highly active ROS (reactive oxygen species) such as O<sub>2</sub>,

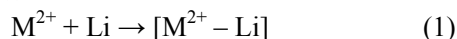
H<sub>2</sub>O<sub>2</sub> and OH· through Haber-Weiss reactions [20]. In general, free transition metal ions have a pivotal role in the generation of oxygen free radical in living organism [21]. The production of these radicals leads to lipid peroxidation, protein modification and DNA damage [22]. The ferrous state of iron accelerates lipid oxidation by breaking down the hydrogen and lipid peroxide to reactive radical via the Fenton reactions [23]. Therefore, the complexation with different divalent metal ions (Mg<sup>2+</sup>, Ca<sup>2+</sup>, Fe<sup>2+</sup> and Cu<sup>2+</sup>) with organic ligands such as 4-benzylidenamino-4,5-dihydro-1H-1,2,4-triazol-5-one derivatives prevent redox cycling [24-25]. However no published data referring to binding of metal by 4-benzylidenamino-4,5-dihydro-1H-1,2,4-triazol-5-one derivatives have been reported.

In the present study, we aim at theoretical investigation of complexations of BDHTD (4-benzylidenamino-4,5-dihydro-1H-1,2,4-triazol-5-one derivatives) by divalent doubly charged metal ions M<sup>2+</sup> (M = Mg, Ca, Fe and Cu) using DFT (density functional theory) [26]. The authors had only approached complexation in bidentate complexes. The substitution effects on the structural geometries of the complexes obtained was also analyzed in gas phase and non-aqueous solvent media (acetonitrile and DMF (N,N-dimethylformamide)). The interaction of BDHTD with Mg<sup>2+</sup>, Ca<sup>2+</sup>, Fe<sup>2+</sup> and Cu<sup>2+</sup> was explored. The electronic structures and the impact of the metal chelation on the antioxidant activity of BDHTD have also been investigated.

## 2. Computational Details

All compounds were optimized with the Gaussian 03 program [27] employing the electron correlated B3LYP functional [27] of the DFT (density functional theory) method [28]. Previous theoretical calculations have shown that the B3LYP approach is a cost-effective method for studying transition metal-ligand systems [28-31]. The polarized double zeta split valence 6-31G(d,p) was chosen and used

throughout the computational process. Vibrational frequency calculations give the zero point vibrational energies and the number of imaginary frequencies. Absolute energies and Gibbs energies were computed for all complexes studied in various media. The NBO (natural bond orbital) technique [32] was used for charge computations. Absolute energies, enthalpies and free energies were computed for the reactions studied (Eq. (1)).



where, Li (i = a, b and c) represents 4-benzylidenamino-4,5-dihydro-1H-1,2,4-triazol-5-one derivative and  $M^{2+}$  is the particular divalent metal ion. Correlation between the MIA (metal ion affinity) and the retained charge (Q/e) of metal ions and that between the former and the HOMO-LUMO (highest occupied molecular orbital-lowest unoccupied molecular orbital) energy gap of  $M^{2+}$ -Li Complexes. The MIA value was assumed to be the negative of the enthalpy change ( $\Delta G_{298}^0$ ) during the complexation process (1). For more quantitative description of the ligand's affinity towards individual cations ( $Mg^{2+}$ ,  $Ca^{2+}$ ,  $Fe^{2+}$  and  $Cu^{2+}$ , respectively), the total selectivity ( $\Delta G_{298}^0$ ) was calculated. The impact of the chelation on the antioxydant activity was investigated through BDE (bond dissociation energy) and the HOMO (highest occupied molecular orbital) eigenvalues of the complexes.

By definition, the BDE of a given X-H bond of the  $M^{2+}$ -Li complex is the enthalpy change of dissociation reaction.



$$BDE = \Delta_f H^0(RX) + \Delta_f H^0(H) - \Delta_f H^0(RX - H) \quad (3)$$

All these calculations were undertaken in vacuum and non-aqueous solvents. Continuum solvation models turned out to be an important tool for investigation of some properties of molecules in solution, due to their relative flexibility and low computational cost. The PCM (polarizable continuum model) presents good accuracy, adaptability and reduced computational effort in describing solvent

effects [33]. Furthermore, PCM method has been widely adopted in the description of the thermodynamic characteristics of salvation [34]. This fact justifies the use of the IEF-PCM (integral formulation version of PCM) throughout this work at the same level of computation.

### 3. Results and Discussion

#### 3.1 Structural Details

Geometry optimizations were performed with two distinct coordination modes:  $k^2$ -N, O and the  $k^2$ -O,O structures. Fig. 1 displays the molecular labels used in this work.

##### 3.1.1 $k^2$ -N,O Structures

The  $k^2$ -N,O optimized structures in gas-phase are presented in Fig. 2. The relevant parameters are given in the Table 1. An inspection of the geometrical parameters of the  $k^2$ -N,O structures reveals that the M-O bonds are always shorter by about 0.030-0.232 Å than the analogous M-N distances. The distances M-N and M-O increase in the same order for R=H: the order observed for R=H is  $5a > 7a > 1a > 3a$ . Whereas, for R =  $CH_3$  and  $C_3H_5$ , the order varies according to the bond considered. For instance for R =  $C_3H_5$ , the increasing of the distances M-O and M-N follows respectively the order:  $7a > 5a > 1a > 3a$  and  $5a > 7a > 1a > 3a$ . In general, the  $M^{2+}$ -BDHTD system shows a larger activation of adjacent bonds of the divalent cation metal, as can be observed in Table 1. The lengthening of the distances C=O compared to the value of free BDHTD can also be observed. The maximum bond length change is obtained for 1a (0.161 Å). The lengthening of the distances  $N_1$ - $N_2$  is also meaningful. In contrast, chelation with divalent metal cations leads to slight shortening of  $C_8$ - $N_2$  ranging between 0.031 and 0.063 Å. The chelate rings of the BDHTD-M (M =  $Mg^{2+}$ ,  $Ca^{2+}$ ,  $Fe^{2+}$  and  $Cu^{2+}$ ) are not planar due to the fact that the metal chelation drastically distorted the BDHTD structures, in which  $M^{2+}$  is coordinated to  $O_1$  atoms with minimum value

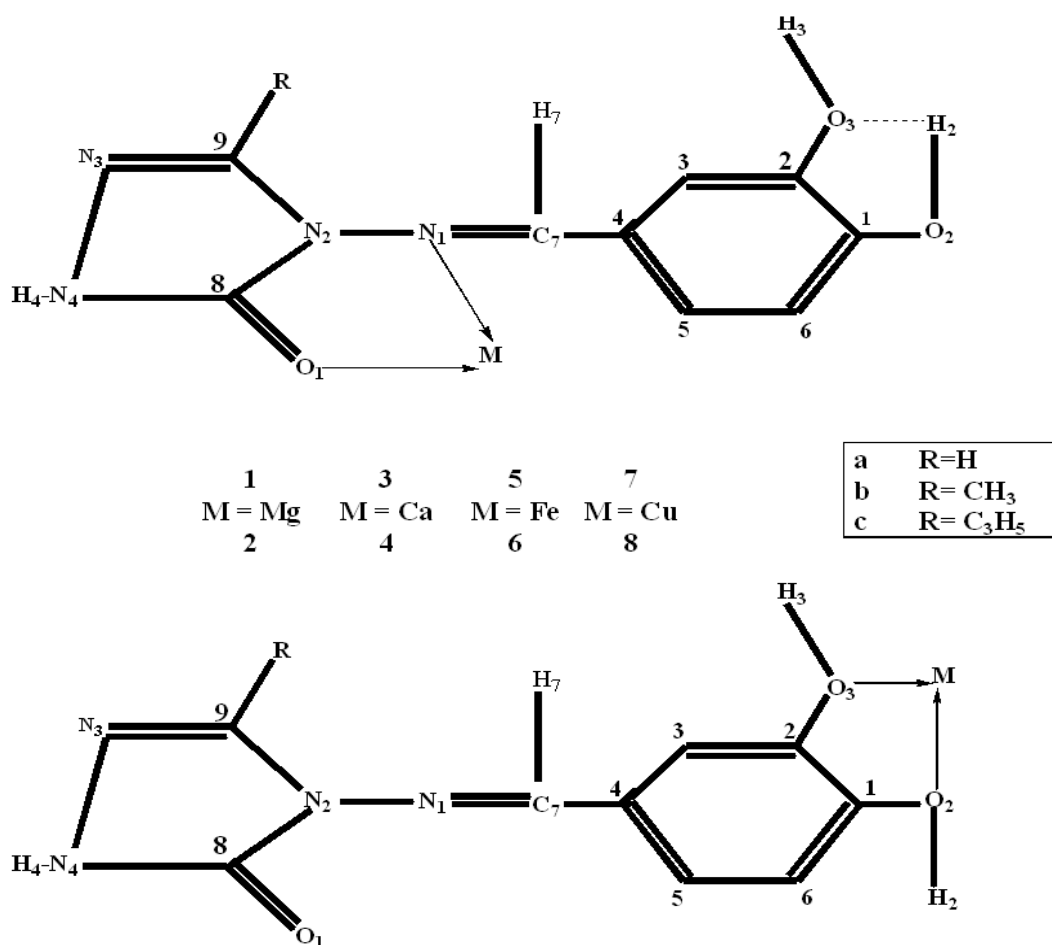


Fig. 1 Numbering system used to identify the bond lengths and angles in  $M^{2+}$ -(4 benzylidenamino-4,5, dihydro-1-H 1,2,4 triazol-5-one derivative complexes: ( $k^2$ -(O,O) structures(above)) and  $k^2$ -(O,N) structures (below)).

Table 1 B3LYP/6-31G(d,p) optimized relevant bond lengths (Å), bonds angles (degrees) and dihedral angles ( $^\circ$ ) for the metal-(4 Benzylidenamino-4,5, dihydro-1-H 1,2,4 triazol-5-one derivative complexes. Upper bold face numbers are calculated in gas phase and lower numbers are calculated in acetonitrile.

		a				b				c					
Parameters		1	3	5	7		1	3	5	7		1	3	5	7
d(M-N <sub>1</sub> )	-	2.051	2.462	1.904	1.908	-	2.095	2.055	1.905	1.901	-	2.052	2.456	1.903	1.898
	-	2.198	2.727	1.936	1.914	-	2.259	2.872	1.940	1.913	-	2.095	2.699	1.931	1.912
d(M-O <sub>1</sub> )	-	1.909	2.230	1.819	1.878	-	1.957	1.911	1.820	1.870	-	1.908	2.225	1.816	1.869
	-	2.024	2.426	1.952	1.867	-	1.994	2.383	1.951	1.870	-	1.957	2.431	1.949	1.867
θ[O <sub>1</sub> -M-N <sub>2</sub> ]	-	87.8	72.8	89.2	91.7	-	80.8	87.9	89.4	91.6	-	87.9	72.9	89.6	91.7
	-	79.9	65.3	85.6	90.0	-	79.9	63.8	85.4	89.8	-	80.8	65.5	85.4	89.8
		2	4	6	8		2	4	6	8		2	4	6	8
d(M-O <sub>2</sub> )	-	2.010	2.325	1.913	1.920	-	2.983	2.651	1.883	1.933	-	2.034	2.350	1.892	1.908
		2.095	2.532	1.911	1.921		2.079	2.518	1.914	1.924	-	3.490	2.523	1.906	1.932
d(M-O <sub>3</sub> )	-	2.007	2.323	1.898	1.910	-	2.893	2.613	1.891	2.258	-	2.031	2.347	1.928	1.905
	-	2.084	2.510	1.910	1.919	-	2.099	2.537	1.909	1.920		3.453	2.490	1.909	1.923
θ[O <sub>2</sub> -M-O <sub>3</sub> ]	-	80.6	70.8	85.1	87.6	-	53.2	59.1	83.7	75.8	-	79.1	69.5	84.1	88.7
	-	75.1	62.1	80.2	84.9	-	75.4	62.0	80.3	84.9	-	45.0	62.738	80.2	84.2
θ[N <sub>2</sub> -N <sub>1</sub> -C <sub>7</sub> -C <sub>4</sub> ]	-7.1	9.4	8.2	-8.8	-15.8	-8.5	8.9	5.2	-10.8	4.9	-8.4	7.9	8.1	0.0	-8.0
	-	-8.6	8.10	-8.4	-11.6	-	8.5	8.3	-8.9	10.9	-	0.0	0.0	0.0	-8.3

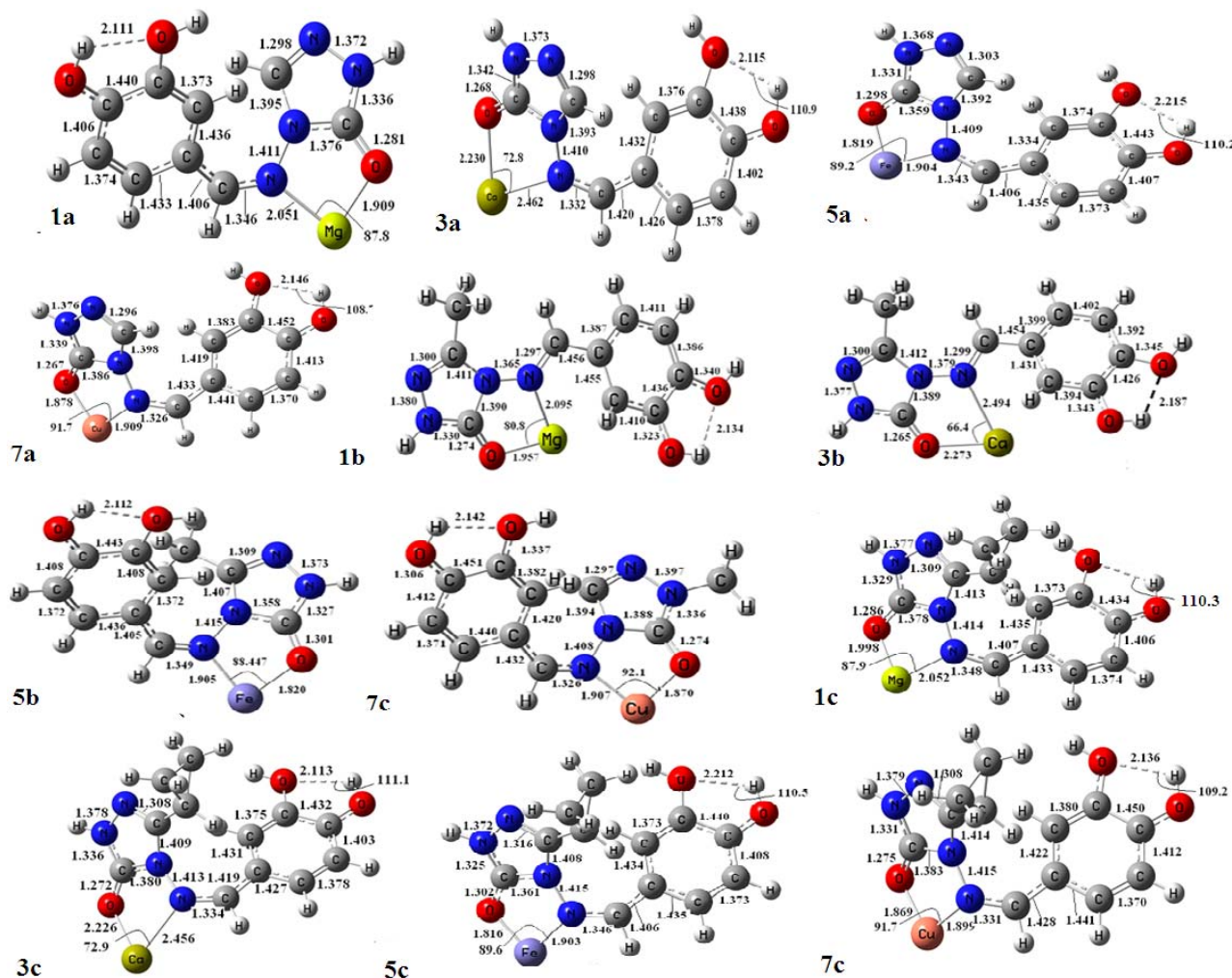


Fig. 2 Optimized  $k^2$ -(O,N) structures (in gas) at B3LYP/6-31G(d,p) of  $M^{2+}$ -(3-methyl-4(3,4-dihydroxybenzylidenamino)-4,5-dihydro-1H-1,2,4-triazol-5-one) complexes  $M = \text{Mg, Ca, Fe and Cu}$  in gas phase.

of  $10.1^\circ$  above the plan  $\text{O}_1\text{C}_8\text{N}_2$ .

The optimized  $\text{N}_1\text{-M-O}_1$  angle in all the transition metal complexes is close to  $90^\circ$  with the highest value observed for  $\text{Cu}^{\text{II}}$  complexes (7a and 7c:  $\text{N-M-O} = 91.7^\circ$ ) and the lowest value for 5a ( $\text{N-M-O} = 89.2^\circ$ ). Each complex presents a intermolecular hydrogen bond  $\text{O}_2\text{-H}_2\cdots\text{O}_3$  between the hydroxyl hydrogen atom  $\text{H}_2$  and hydroxyl oxygen atom  $\text{O}_2$ . The hydrogen bond lengths in all the complexes are highly influenced by the metal chelation. The maximum bond length difference obtained from free BDHTD structures is equal to  $0.08 \text{ \AA}$  (for 1c). For all complexes, the hydrogen bond distances are less than  $3.0 \text{ \AA}$  while the  $\text{O}_2\text{-H}_2\cdots\text{O}_3$  bond angles are more than  $110^\circ$ . This is in agreement with the definition of the hydrogen bond [35, 36].

Independently from the substitution, the bond lengths of the triazol ring are also highly affected by the metal chelation. Nonetheless, the amide  $\text{C}_8\text{-N}_4$  bond length values are intermediate between the single bond length of  $1.470 \text{ \AA}$  and the double length of  $1.240 \text{ \AA}$  [37, 38].

The impact of the metal chelation on the planarity of the triazol ring in all the complexes is minor: the  $\theta[\text{C}_8\text{-N}_2\text{-C}_9\text{-N}_3]$  dihedral angle value ranges between  $0.3^\circ$  and  $7.6^\circ$ . The mean planes through the triazol ring and phenyl ring form a dihedral angle ranging between  $5.3^\circ$  and  $17.8^\circ$ . The geometrical disturbance induced by the metal chelation does not extend significantly beyond the bond lengths of phenyl ring. Collectively, the phenyl ring remains in a planar form.

The geometrical parameters obtained after the

solvation of the molecular system are almost identical when using acetonitrile and DMF as solvent. This fact explains why the results estimated in the latter one are not reported. In general, the author's data show a sensible elongation of bond distances around the metal

atom. For instance, differences in  $M-X_1$  ( $X = O, N$ ) bond lengths are in the range 0.004-0.243 Å. Nevertheless, except for 1c and 3c complexes, Fig. 3 exhibits a shorting of the hydrogen bond length. non-aqueous solvents.

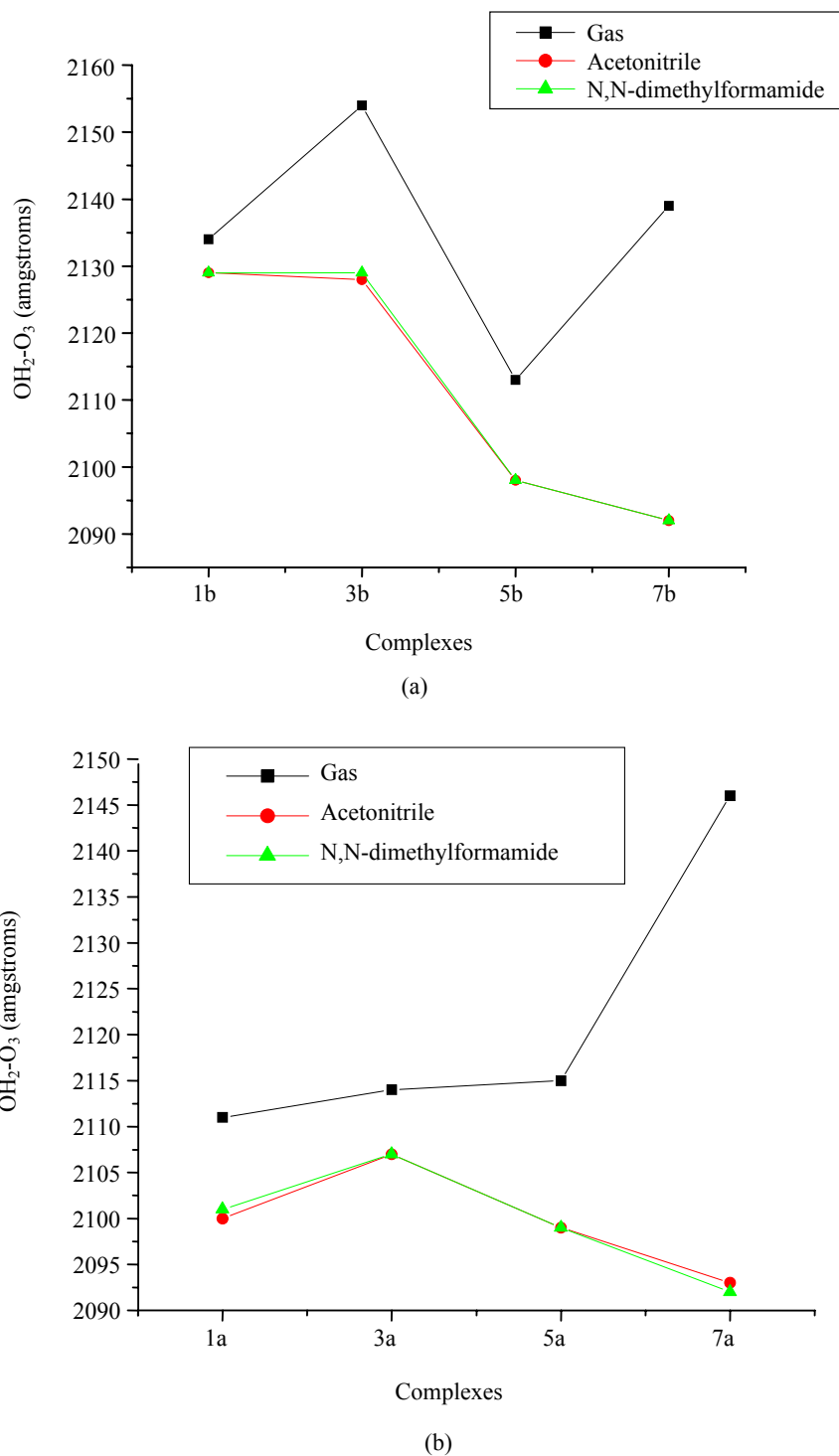


**Fig. 3** Hydrogen bond lengths of optimized  $k^2-(O,N)$  structures in various media.



3.1.2  $k^2$ -O,O Structures

Fig. 4 shows the obtained minima for  $k^2$ -O,O structures. The complexation of BDHTD by divalent metal cations ( $Mg^{2+}$ ,  $Ca^{2+}$ ,  $Fe^{2+}$  and  $Cu^{2+}$ ) induce a slight change of structural parameters in the side chain between the phenyl ring and triazole homolog. The maximum bond length and bond angles are 0.063 Å and  $5.5^\circ$ , respectively. These maximum values correspond to the chelation with  $Fe^{2+}$ . The impact of chelation on the structural parameters of the two rings is also minor. Contrary to the  $k^2$ -N,O structures, the coordination mode  $k^2$ -O,O only affect the site of chelation. The previous examination of chelation of phenolic acids by divalent metal cations with 'OH radical confirms this localised strong geometrical disturbance [39]. Nevertheless, it is worth noting that the values of the  $C_2-O_3$ ,  $C_1-O_2$ ,  $O_3-H_3$  and  $O_2-H_2$  bonds do not vary considerably. For instance, the authors' calculations show bond length difference

lengthening of C-O bonds in different complexes in the range: 0.01-0.071 Å. This may result from the absence of highly active ROS (reactive oxygen species) such 'OH in the authors' model. It may also be seen that, in most case, the divalent metal cation attaches to the phenolic group with two metal-oxygen bonds of almost similar lengths, except in the cases of 4b, 8b and 6c, in which the  $M^{2+}$  are strongly non-symmetrical. The  $O_2-M-O_3-C_2$  dihedral angles values, which range from  $0.0^\circ$  to  $5.7^\circ$ , reveal that the chelate ring of BDHTD...M ( $M = Mg^{2+}$ ,  $Ca^{2+}$ ,  $Fe^{2+}$  and  $Cu^{2+}$ ) complexes are almost planar. From calculated results, it can be found that the whole molecule is almost planar and the two rings show a dihedral angle in the range:  $0.0^\circ$ - $15.8^\circ$ . The authors' data also illustrate that the triazole and benzene rings are nearly planar. For complexes 2b, 4b and 8b, the planarity of the molecule is maintained by the intermolecular hydrogen bonds  $C_8-O_1...HC_1$ . Except

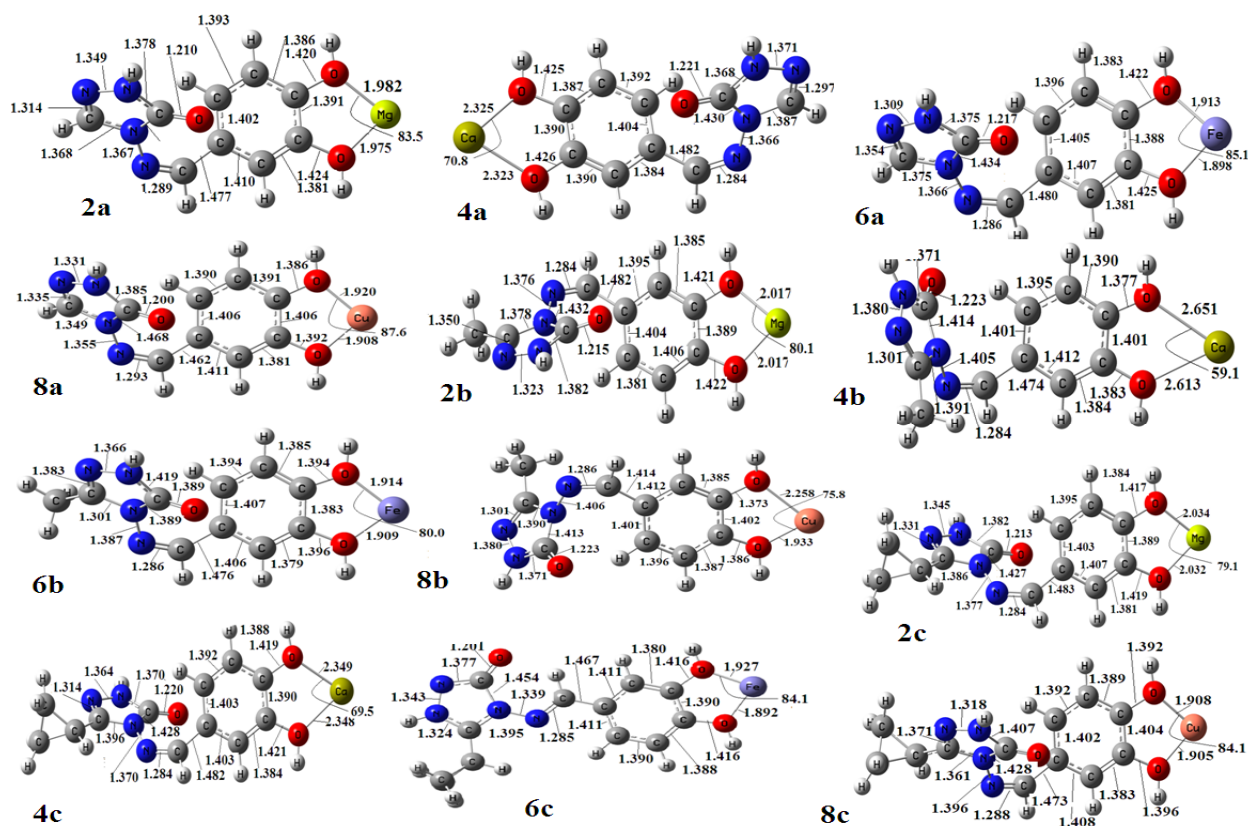


Fig. 4 Optimized  $k^2$ -(O,O) structures (in gas) at B3LYP/6-31G(d,p) of  $M^{2+}$ -(3-methyl-4(3,4-dihydroxybenzylidenamino)-4,5, dihydro-1-H 1,2,4 triazol-5-one) complexes  $M = Mg, Ca, Fe$  and  $Cu$  in gas phase.

for 6c complex, the chelation effect slightly affected the values of  $N_2-N_1-C_7-C_4$  dihedral angles of BDHTD.

The variation of these dihedral angles shows that solvation of complexes lead to structures with phenyl and triazole rings contained in the same plane for 2c, 4c and 6c complexes. The impact of solvation on the geometrical structures is very sensitive. For example, differences in M-O<sub>1</sub> bond lengths, for example were in the range: 0.001-1.456 Å.

### 3.2 Stability and Interaction Energies

The total energies and the relative free energies of our series of 24 complexes calculated in various media are given in Table 4. In general, the most stable  $M^{2+}$ -BDHTD complexes are the  $k^2$ -N,O structures in

gas phase. This trend remains constant for the ligand a in acetonitrile and DMF. However, for the ligands b and, the  $k^2$ -O,O structures are more stable for c with divalent metal cations  $M^{2+}$  (M = Mg and Ca) in acetonitrile and with  $Ca^{2+}$  in DMF. For each coordination mode, the stability increases with the increasing of the atomic number of the divalent metal cation  $M^{2+}$ . The geometry optimizations in the used non-aqueous solvent indicate that the solvation of complexes significantly increases of the stability except for 6c complex. The energy gap between data in gas phase and in solution is in the range: 153.1-399.7 and 59.6-266.5 kcal·mol<sup>-1</sup>, respectively for acetonitrile and DMF. Close inspection of author's data reveals the enhancement of the stability when the number of the carbon atom of the substituent (R)

**Table 2** Total electronic energies and relative free energies of the metal-4 Benzylidenamino-4,5, Dihydro-1-H 1,2,4 triazol-5-one derivative complexes ( $T = 298.15$  K) computed in various media using B3LYP/6-31G\*\*.

	Electronic energy (Hartree <sup>a</sup> )			Relative free energy (kcal·mol <sup>-1</sup> )		
	Gas	Acetonitrile	DMF	Gas	Acetonitrile	DMF
1a	-991.96471	-992.32573	-992.32627	86.0	95.9	95.6
2a	-991.89831	-992.30186	-992.125629	82.9	94.1	84.2
3a	-1,469.49176	-1,469.86636	-1,469.86697	84.9	93.4	94.3
4a	-1,469.43354	-1,469.85325	-1,469.677518	81.9	82.7	82.7
5a	-2,055.32234	-2,055.65706	-2,055.65756	85.5	95.5	95.4
6a	-2,055.24053	-2,055.58416	-2,055.407016	85.2	94.9	84.9
7a	-2,432.08671	-2,432.36278	-2,432.36316	84.4	95.0	94.9
8a	-2,432.04188	-2,432.31275	-2,432.136917	81.1	92.9	82.8
1b	-1,031.32875	-1,031.65905	-1,031.63128	102.5	172.7	102.6
2b	-1,031.23268	-1,031.63067	-1,031.426651	99.1	170.4	100.4
3b	-1,508.86884	-1,509.20011	-1,509.18210	100.8	95.7	99.6
4b	-1,508.76598	-1,509.18149	-1,508.977915	98.3	99.7	99.5
5b	-2,094.65497	-2,094.98259	-2,094.91286	101.8	102.0	172.0
6b	-2,094.55080	-2,094.91229	-2,094.708039	99.1	100.2	100.2
7b	-2,471.41884	-2,471.69026	-2,471.69064	100.8	101.3	171.2
8b	-2,471.38244	-2,471.64299	-2,471.64338	96.6	99.2	99.2
1c	-1,108.68790	-1,108.68789	-1,109.03833	122.0	122.1	122.2
2c	-1,108.62909	-1,108.99711	-1,108.99787	122.0	119.6	118.5
3c	-1,586.21255	-1,586.57823	-1,586.57877	121.0	119.0	120.5
4c	-1,586.15638	-1,586.58048	-1,586.58108	118.2	118.6	118.8
5c	-2,172.04849	-2,172.36970	-2,172.37019	121.5	121.5	122.5
6c	-2,171.93290	-2,172.29596	-2,172.30645	119.8	121.0	120.7
7c	-2,548.81109	-2,549.07692	-2,549.07729	120.2	121.7	121.6
8c	-2,548.78603	-2,549.03000	-2,549.03037	118.0	118.5	118.3

<sup>a</sup>: Dimethylformamide.



increases for complexes with the same central metal. From our calculations, the  $k^2\text{-O,N}$  structures are slightly higher in free energy than the  $k^2\text{-O,O}$  ones in various media, except for complexes of  $\text{Ca}^{2+}$  with ligand b. This fact shows the preference of divalent metal cations  $\text{M}^{2+}$  ( $\text{M} = \text{Mg}, \text{Ca}, \text{Fe}$  and  $\text{Cu}$ ) to adopt the  $k^2\text{-N,O}$  dicoordination mode.

The interaction energies  $D_e$ , enthalpies ( $\Delta H_{298}^0$ ) and Gibbs energies of the complexation process (1) studied computed at B3LYP level calculations in various media are given in the Table 3. The ZPVE (zero-point vibration energy) corrections are applied

in the present case. The computed interaction energies values for ligand a at CCSD(T) level are also inserted in Table. 3. The comparison between the CCSD(T) and B3LYP results shows that the B3LYP interaction energy are lower than the CCSD(T) ones. Constantino et al. [40] discussed on the interaction of  $\text{Co}^+$  and  $\text{Co}^{2+}$  with glycine, and their calculations confirmed this fact especially for divalent metal cations. Koch et al. [41] attributed such a larger interaction energy difference to the tendency of the DFT methods to overstabilize the d-d exchanage. From author's data, one can observe that the impact of substitution of hydrogen atom by

**Table 3** Interaction energies ( $D_e$ ,  $\Delta H_{298}^0$  and  $\Delta G_{298}^0$  (kcal·mol<sup>-1</sup>)) for ions  $\text{ML}^{2+}$  in various media using B3LYP/6-31G(d,p). Bold face numbers are calculated in gas phase at CCSD(T) level.

*Li		M = Mg		M = Ca		M = Fe		M = Cu			
		1	2	3	4	5	6	7	8		
a	D <sub>e</sub>	Gas	-581.5	-807.7	-555.5	-521.5	-461.2	-663.7	-711.9	-906.5	
			-213.8	-159.4	-147.4	-102.7	-173.7	-87.2	-217.4	-204.2	
		Acetonitrile	-4.0	-16.5	-13.2	-5.9	-263.7	-40.6	-114.9	-86.1	
		DMF	-30.7	-17.7	-13.1	-5.9	-85.3	-40.5	-114.7	-85.9	
	ΔH <sub>298</sub> <sup>0**</sup>	Gas	-627.2	-588.4	-556.9	-584.7	-462.9	-375.7	-713.6	-688.3	
		Acetonitrile	-32.4	-19.0	-14.3	-6.8	-284.5	-42.1	-73.7	-44.6	
		DMF	-32.2	-18.9	-14.3	-6.7	-86.8	-41.9	-73.7	-44.6	
	ΔG <sub>298</sub> <sup>0**</sup>	Gas	-625.1	-589.6	-537.0	-506.4	-692.6	-728.9	-692.5	-670.9	
		Acetonitrile	-12.9	-1.6	-87.9	-94.7	-143.3	-22.2	-18.7	-8.5	
		DMF	-12.0	-1.6	-3.9	8.9	-67.1	-22.2	-18.8	8.4	
	b	D <sub>e</sub>	Gas	-227.9	-169.1	-166.7	-103.4	-294.3	-234.3	-42.6	-274.0
			Acetonitrile	-34.0	-18.0	-16.8	-5.7	-83.6	-44.1	-144.4	87.1
DMF			-33.8	-17.9	-19.7	-5.7	-83.4	-40.9	-114.2	-86.2	
ΔH <sub>298</sub> <sup>0**</sup>		Gas	-229.7	-40.2	-167.9	-104.4	-295.9	-235.5	-44.1	-275.0	
		Acetonitrile	-35.6	-19.0	-17.8	-6.7	-81.9	-42.4	-73.3	-45.7	
		DMF	-315.7	-19.0	-17.7	-6.7	-85.0	-42.2	-73.2	-45.6	
ΔG <sub>298</sub> <sup>0**</sup>		Gas	-227.6	-437.4	-148.6	-89.2	-275.4	-218.0	-274.9	-659.1	
		Acetonitrile	-15.8	-1.8	-84.5	-96.0	-64.4	-23.9	-18.1	-7.3	
		DMF	-15.0	-1.7	-1.4	10.1	-64.7	-24.2	-18.1	7.3	
c		D <sub>e</sub>	Gas	-62.3	-53.0	-9.1	-41.8	-149.7	-406.2	-162.1	-434.7
			Acetonitrile	-328.1	-130.7	356.5	-123.5	-53.8	-98.8	-23.3	-49.9
			DMF	108.5	131.4	126.2	126.3	54	92.6	152.2	50.2
	ΔH <sub>298</sub> <sup>0**</sup>	Gas	-74.4	-4.0	-2.7	-30.3	-161.9	-441.1	-163.2	-147.9	
		Acetonitrile	-326.5	-129.4	-355.1	-122.8	-52.2	-97.4	-64.4	91.5	
		DMF	107.1	130.6	122.9	122.8	52.4	91.3	64.4	91.6	
	ΔG <sub>298</sub> <sup>0**</sup>	Gas	-73.9	-42.2	-15.9	-45.5	-142.4	-99.0	-143.1	-131.1	
		Acetonitrile	-345.9	-147.0	-459.8	-224.6	-73.9	-116.9	-120.6	-143.7	
		DMF	126.9	144.7	143.2	138.7	73.5	110.2	120.4	143.1	

\*Li: Corresponds to 4 Benzylidenamino-4,5. Dihydro-1-H 1,2,4 triazol-5-ones derivatives.

\*\* : After taking into account thermal corrections at B3LYP/6-31G(d,p).

$\text{CH}_3$  and  $\text{C}_3\text{H}_5$  does not affect the CCSD(T) values. Both methods predict almost the higher interaction energies of  $k^2\text{-N,O}$  structures. In non-aqueous media, a notable rise of interaction energies is observed, except for complexes of  $\text{M}^{2+}$  ( $\text{M} = \text{Mg}$  and  $\text{Ca}$ ) with ligand c. This rise is due to the collision between solute and solvent molecules.

When looking at the heat of complexation in gas phase, we note that the MIA (metal ion affinity) highly varies with the coordination mode and substitution effect. For instance, with  $k^2\text{-N,O}$  structures, the MIA decreases in the order:  $\text{Cu}^{2+} > \text{Fe}^{2+} > \text{Mg}^{2+} > \text{Ca}^{2+}$  for the ligand c controversially, the order observed for the ligand b is  $\text{Fe}^{2+} > \text{Mg}^{2+} > \text{Ca}^{2+} > \text{Cu}^{2+}$ . The solvent effect on the MIA is very versatile. To see the possible correlation between the retained charge of divalent metal(II) cations and MIA value. The two parameters are plotted for each ligand (Fig. 5). For the ligand a, MIA values vary inversely with the retained charge of metal ion, except for copper(II) complexes. The same trend is globally observed for the ligand c, except for iron(II) and copper(II) cations in  $k^2\text{-O,O}$  coordination mode. This exception is also made for iron(II) complexes (5b and 6b) and copper(II) complex (8b) for the ligand b. This possible correlation between the MIA and retained charge of metal was confirmed by previous works focused on the DFT study of interaction of thymine with  $\text{Cu}^+$  and  $\text{Zn}^{2+}$  [42, 43].

The sign of the values of Gibb energies for the reaction of complexation (1) shows that the complexation is possible in gas and in acetonitrile. In DMF, the complexation with the ligand c is impossible. In the same way, the complexation in the  $k^2\text{-O,O}$  coordination mode with the ligands a and b is also impracticable with divalent copper(II) cation in this solvent. The chelation of divalent calcium cation ( $\text{Ca}^{2+}$ ) by ligand b in this solvent cannot take place. For a more quantitative description of the ligand's affinity toward individual cations ( $\text{Mg}^{2+}$ ,  $\text{Ca}^{2+}$ ,  $\text{Fe}^{2+}$  and  $\text{Cu}^{2+}$ , respectively), the total selectivity ( $\Delta G_{298}^0$ )

was calculated as the difference between the Gibbs complexation energies of  $\text{Cu}^{2+}$  and  $\text{Ca}^{2+}$ ,  $\text{Fe}^{2+}$  and  $\text{Ca}^{2+}$  and  $\text{Mg}^{2+}$  and  $\text{Ca}^{2+}$  (Table 4). The analysis of the total selectivity was limited to more stable  $k^2\text{-N,O}$  structures. In real situation, a complete solvent shell surrounds the ion. Due to the lack of solvation shell, the authors have only focused the selectivity effect in gas phase. The differences in the selectivity for  $\text{Ca}^{2+}$  ion over the transition metal cations ( $\text{Fe}^{2+}$  and  $\text{Cu}^{2+}$ ) show that the ligand c and b are seen to be the least discriminatory ligands by having the smallest magnitude for the complexes of cations. The absolute values of  $\Delta G^{298}$  indicate that the  $\text{Cu}^{2+}$  is about 127-134  $\text{kcal}\cdot\text{mol}^{-1}$  more selected than  $\text{Ca}^{2+}$ . Much higher selectivity is exhibited by  $\text{Fe}^{2+}$  cation (about 127-156  $\text{kcal}\cdot\text{mol}^{-1}$ ).

### 3.3 Bond dissociation Energy and electronic structures

The variation of the bond dissociation energies of  $\text{X-H}_n$  ( $\text{X} = \text{O}, \text{C}$ ;  $n = 2, 3, 4, 7$ ) is almost identical. For sake of simplicity, the bond dissociation energies for  $\text{O}_2\text{-H}_2$  of BDHTD (b and c) only are presented in Table 5. The comparison of BDEs in both coordination modes shows that the decrease in  $\text{BDE}_2$  was more pronounced for  $k^2\text{-O,O}$  coordination mode, exception made for  $\text{Cu}^{2+}$  complexes. The calculated BDE values of the  $k^2\text{-O,O}$  complexes decreases when one goes from BDHTD to  $\text{M}^{2+}\text{-BDHTD}$  complexes, demonstrating clearly that the antioxidant efficiency of BDHTD was enhanced by the chelation of BDHTD particularly for  $k^2\text{-O,O}$  coordination mode. This decrease is more important for  $\text{Mg}^{2+}$ ,  $\text{Ca}^{2+}$  and  $\text{Fe}^{2+}$ , but less important for  $\text{Cu}^{2+}$ . This fact is in agreement with hydrogen transfer in the reaction of metal associated to phenolic acids analyzed by Fifen et al. [39]. The higher the HOMO eigenvalue is, the higher the antioxidant activity is. The author's results revealed that higher  $E_{\text{HOMO}}$  values are obtained for  $k^2\text{-O,O}$  coordination. In both coordination modes, the enhancement of the antioxidant activity by the

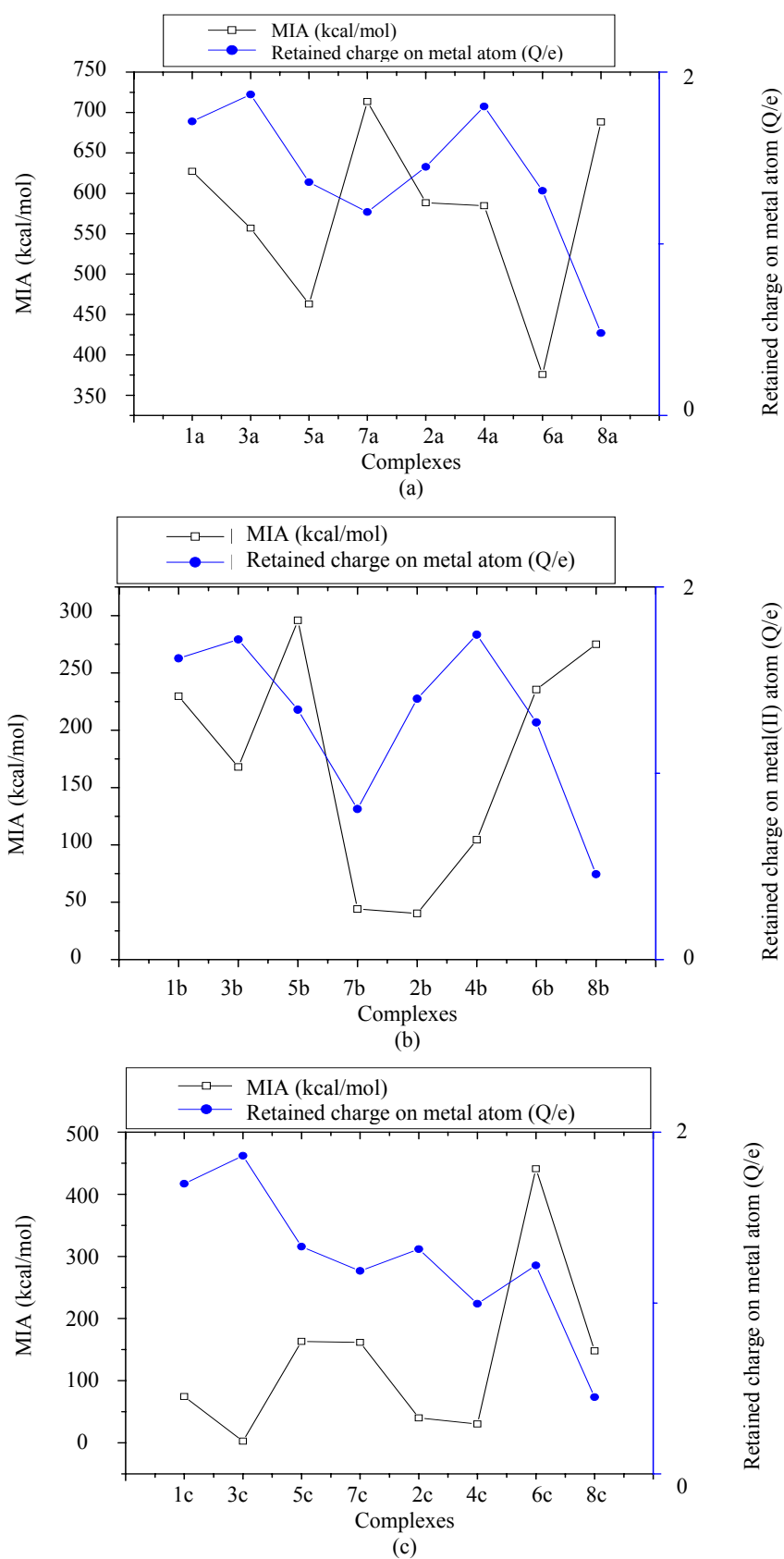


Fig. 5 Correlation between the MIA ( $\text{kcal}\cdot\text{mol}^{-1}$ ) and retained charge (Q/e) of Mg (in gas).

transition metal chelation decreases in the following order:  $\text{Ca}^{2+} > \text{Mg}^{2+} > \text{Fe}^{2+} > \text{Cu}^{2+}$ . The ordering of the antioxidant activity done on the basis of  $E_{\text{HOMO}}$  values was consistent with the one obtained using BDE for  $k^2\text{-O}_2\text{O}$  coordination mode.

The correlation agrees with the conclusion of previous works [44, 45] that showed the correlation between the BDE and HOMO values.

### 3.4 Charge Transfer Induced by Metal Chelation

The natural charge distribution of atoms in gas-phase has been performed on the gas-phase geometries at the same basis level. The charge on metal atom is also listed in Table 5. Our results show that the net charge on the metal atom is lower for  $k^2\text{-(O,O)}$  complexes. The  $k^2\text{-(O,O)}$  coordination mode highly alter the redox potential of metal atom and render them more inactive. This confirms the fact that such a coordination mode leads to complexes with higher antioxidant activities. The calculations yielded the net charge carried by the metal ion of the  $k^2\text{-(O,O)}$  complex formed in the range:  $+(1.32\text{--}1.45)e$ , for magnesium atom,  $+(1.74\text{--}1.80)e$  for calcium atom,

$+(1.22\text{--}1.31)e$  for iron atom and  $+(0.45\text{--}0.93)e$  for copper atom. Our results are in good agreement with previous in investigation on phenolic acid [39] that revealed that the metal ion has undergone a reduction while the whole substrate has undergone an oxidation. One can then conclude that the NBO analysis is a valuable approach for investigation of charge transfer (in a chemical compound) from the substrate to metal ion which increases with the electronegativity of the metal ion. This result is consistent the observations done on quercetin [46] and on phenolic acids [39]. The ability of entrapment of transition metal ion ( $\text{Mg}^{2+}$ ,  $\text{Ca}^{2+}$ ,  $\text{Fe}^{2+}$  and  $\text{Cu}^{2+}$ ) by BDHTD afterwards prevent these from participating in free free radicals generation [21].

## 5. Conclusions

Transition metal (II) complexes of 4-benzylidenamino-4,5-dihydro-1H-1,2,4-triazol-5-one derivatives were studied by the means of density functional theory to give better insight into the effect of metal chelation on antioxidant properties. Two plausible structures of two distinct coordination

**Table 4** Selectivity from binding Gibbs energy ( $\Delta G^{298}$ , kcal·mol<sup>-1</sup>) for divalent metal cations  $\text{M}^{2+}$  ( $\text{M} = \text{Ca}, \text{Fe}$  and  $\text{Cu}$ ) over  $\text{Mg}^{2+}$  in gas phase.

Li	$\text{Mg}^{2+}$ over $\text{Ca}^{2+}$	$\text{Fe}^{2+}$ over $\text{Ca}^{2+}$	$\text{Cu}^{2+}$ over $\text{Ca}^{2+}$
a	-88.1	-155.6	-133.9
b	-79.0	-126.8	-126.3
c	-58.0	-126.5	-127.2

\*Li: Corresponds to 4 Benzylidenamino-4,5. Dihydro-1-H 1,2,4 triazol-5-ones derivatives.

**Table 5** Bond dissociation ( $\text{BDE}_2$ ) for single hydrogen atom transfer at B3LYP level, HOMO eigenvalue (ev) and NBO charge (q/e) carried by the metal ion in gas phase.

*Li		1	2	3	4	5	6	7	8	
a	-E <sub>HOMO</sub>	5.8	12.9	12.2	12.2	11.2	13.2	12.3	13.6	12.6
	q/e	-	1.7	1.45	1.87	1.80	1.36	1.31	1.19	0.93
	BDE <sub>2</sub> <sup>**</sup>	82.0	86.3	25.5	98.4	28.2	-	34.7	57.9	72.1
b	-E <sub>HOMO</sub>	5.7	13.5	11.9	13.1	11.0	13.2	12.1	13.9	12.3
	q/e	-	1.62	1.40	1.72	1.74	1.34	1.27	0.81	0.91
	BDE <sub>2</sub> <sup>**</sup>	72.7	90.1	24.1	97.5	26.3	-	30.8	88.3	60.7
c	-E <sub>HOMO</sub>	6.0	12.7	11.2	11.9	10.7	13.0	11.2	13.4	11.4
	q/e	-	1.70	1.32	1.86	1.70	1.33	1.22	1.19	0.45
	BDE <sub>2</sub> <sup>**</sup>									

\*Li Corresponds to 4 Benzylidenamino-4,5. Dihydro-1-H 1,2,4 triazol-5-ones derivatives.

\*\* The numeric subscript n= 2 used conjointly for BDE associated to the bonds  $\text{O}_2\text{-H}_2$ .

modes:  $k^2\text{-N, O}$  and the  $k^2\text{-O, O}$ , O have been characterized using DFT methods. The calculations were performed in gas-phase and in solution-phase (acetonitrile, DMF). The optimized  $k^2\text{-N, O}$  complexes present an intermolecular hydrogen bond  $\text{O}_2\text{-H}_2\cdots\text{O}_3$  between the hydroxyl hydrogen atom  $\text{H}_2$  and hydroxyl oxygen atom  $\text{O}_2$ . The geometrical disturbance induced by the metal chelation in this coordination mode does not affect significantly the bond lengths of phenyl ring. Whereas, the bond lengths of the triazol ring are highly altered by the metal chelation. But, the analysis of the  $k^2\text{-O, O}$  optimized structures shows that the geometrical disturbance is only localised on the chelation site. In both cases, the solvation lead to a sensitive elongation of the bond distances.

In gas-phase the  $k^2\text{-N,O}$  structures are the most stable. This trend remains identical for the ligand in a solution-phase. For the others ones, the stability depend on the ligand and on the solvent. In general, the stability increases with the increasing of the atomic number of the divalent metal cation  $\text{M}^{2+}$ . The MIA highly varies with the coordination mode and substitution effect. From the sign of the value of Gibb energies for the complexation, one can conclude that the complexation is possible in gas and acetonitrile. The analysis of selectivity reveals that much higher selectivity is observed by  $\text{Fe}^{2+}$  cation.

Our results shows that the metal chelation decreases the BDE of  $\text{X-H}_n$  ( $n = 2, 3, 4, 7$ ). This reduce of BDEs is more pronounced for  $k^2\text{-O,O}$  complexes. The results corroborate previous works on phenolic acid [39] which revealed that the metal chelation increases the antioxidant activities of compounds. The author's results also revealed that higher  $E_{\text{HOMO}}$  values are obtained for  $k^2\text{-O,O}$  coordination. In both coordination modes, the enhancement of the antioxidant activity by the transition metal chelation decreases in the following order:  $\text{Ca}^{2+} > \text{Mg}^{2+} > \text{Fe}^{2+} > \text{Cu}^{2+}$ .

Moreover, from the natural charge distribution of atoms in gas-phase, one can observe that the net

charge on the metal atom is lower for  $k^2\text{-(O,O)}$  complexes. The  $k^2\text{-(O,O)}$  coordination mode highly alter the redox potential of metal atom and render them more inactive. This confirms the fact that such a coordination mode leads to complexes with higher antioxidant activities.

## Acknowledgements

This investigation was supported by the Ministry of Higher Education of Cameroon. The authors are grateful to Dr. Kenfack Cyril Assongo (Cepamog, University of Douala) for help with calculations.

## References

- [1] Amir, M., and Kumar, S. 2007. *Acta Pharma*. 57: 31.
- [2] Unver, Y., Dugdu, E., Sancak, K., Er, M., and Karaoglu, S. A. 2009. *Turk. J. Chem*. 33: 135.
- [3] Unver, Y., Dugdu, E., Sancak, K., Er, M., and Karaoglu, S. A. 2008. *Turk. J. Chem*. 32: 441.
- [4] Turan-Zitouni, G., Kaplancikli, Z., Erol, K., and Kilic, F. S. 1999. *Il Farmaco* 54: 218.
- [5] Sancak, K., Unver, Y., and Er, M. 2007. *Turk. J. Chem*. 31: 125.
- [6] Emilsson, H., Salender, H., and Gaarder, J. 1985. *Eur. J. Med*. 21: 333.
- [7] Kritsanida, M., Mouroutsou, A., Marakos, P., Pouli, N., and Papakonstantinou-Garoufalias, C. M. 2002. *Il Farmaco* 57: 253.
- [8] Holla, B. S., Poorjary, K. N., Rao, B. S., and Shivananda, M. K. 2002. *Eur. J. Med. Chem*. 37: 511.
- [9] Foroumadi, A., Soltani, F., Moshafi, M. H., and Ashraf-Askari, R. 2003. *Il Farmaco* 58: 1023.
- [10] Mir, I., and Siddiqui, M. T. 1970. *Tetrahedron* 26: 5235.
- [11] Matysiak, J. 2006. *Chem Pharm Bull* 54: 988.
- [12] Yüksek, H., Demibaş, A., İkizler, A., Johansson, C. B., Çelik, C., and İkizler, A. A. 1997. *Arzneim.-Forsch./Drug Res*. 47: 405.
- [13] Mustaffer, A., Yüksek, H., İslamoğlu, F., Bahçeci, Ş., Elamasta, Ş. M. M., Akşit, H., et al. 2007. *Molecules* 12: 1805.
- [14] Yüksek, H., Bahçeci, Ş., Ocak, Z., Alkan, M., Ermiş, B., Mutlu, T., et al. 2004. *Indian J. Heterocycl. Chem*. 13: 369.
- [15] Bahçeci, Ş., Yüksek, H., Ocak, Z., Azakli, I., Alkan, M., and Özdemir, M. 2002. *Collect Czech Chem Commun*. 67: 1215.
- [16] İkizler, A. A., İkizler, A., Şentürk, H. B., and Serdar, M. 1998. *Doğa-Tr Kimya D*. 12: 57.

- [17] Yüksek, H., Kolaylı, S., Küçük, M., Yüksek, O. M., Ocak, U., Şahinbaş, E., et al. 2006. *Indian J Chem.* 45: 715.
- [18] Bikélé, M. D., Zobo, M. J., Lissouck, D., Younang, E., Nono, J. H., and Mbaze, M. L. Unpublished Results.
- [19] Leopoldini, M., Russo, N., Chiodo, S., and Toscano, M. 2006. *J. Agric. Food Chem.* 54: 6343.
- [20] Strlic, M., Radovic, T., Kolar, J., and Pihlar, B. 2002. *J. Agri. Food. Chem.* 50: 6313.
- [21] Brown, J. E., Khodr, H., Hider, R. C., and Rice-Evans, C. A. 1998. *Biochem. J.* 330: 1173.
- [22] Schulz, J. B., Lindenau, J., Seyfried, J., and Dichganz, J. 2000. *Eur. J. Biochem.* 267: 4904.
- [23] Van, A. S. A. B. E., Van, D. B. D. J., Tromp, M. N. J. L., Griffaen, D. H., Van, B. W. P., Van, V. W. J. F., et al. 1996. *Free Radic. Bio. Med.* 20: 331.
- [24] Finefrock, A. E., Bush, A. I., and Doraiswamy, P. M. 2003. *J. Am. Geriatr. Soc.* 51: 1143.
- [25] Gordon, M. H. 1990. *Food Antioxidants*. London: Elsevier.
- [26] Parr, R. G., and Yang, W. 1989. *Density Funtional Theory of Atoms and Molecules*. Oxford University: Oxford Sciences Publications.
- [27] Frisch, M. J., Trucks, G. W., Schlegel, H. B., Scuseria, G. E., Robb, M. A., Cheeseman, J. R., et al. 2010. *Gaussian 09, Revision C..* Wallingford: Gaussian, Inc..
- [28] Holthausen, M. C., Mohr, M., and Koch, W. 1995. *Chem. Phys. Lett.* 240: 245.
- [29] Blomberg, M. R. A., Siegbahn, P. E. M., and Svenssom, M. 1996. *J. Chem. Phys.* 104: 9546.
- [30] Bauschlicher, M. C., Ricca, A., Partridge, H., and Langhoff, S. R. 1997. *Recent Advances in Density Functional Theory*. Singapore: World Scientific Publising Co.
- [31] Luna, A., Alcamí, M., Mó, O., and Yáñez, M. 2000. *Chem. Phys. Lett.* 320: 129.
- [32] Lee, C., Yang, W., and Parr, R. G. 1988. *Phys. Rev. B.* 37: 785.
- [33] Reed, A. E., Weinstock, R. B., and Weinhold, F. 1985. *J. Chem. Phys.* 83: 735.
- [34] Cancès, E., Mennucci, B., and Tomasi, J. 1997. *J. Chem. Phys.* 107: 3022.
- [35] Cossi, M., Rega, N., Scalmani, G., and Barone, V. 2003. *J. Comp. Chem.* 24: 669.
- [36] Steiner, T., and Desiraju, G. R. 1998. *Chem. Commun.* 8: 891.
- [37] Steiner, T. 2002. *Angew. Chem. Int.* 41: 48.
- [38] Robin, M. B., Bovey, F. A., and Basch, H. 1970. *The Chemistry of Amides*. London: Interscience Publishers.
- [39] Jalal, A., Mustafa, M., Musa, Z. N., Kais, A. K. E., and Boese, R. 2003. *Org. Biomol. Chem.* 1: 1798.
- [40] Fifen, J. J., Nsangou, M., Dhaouadi, Z., Motapon, O., and Lahmar, S. 2009. *J. Mol. Struct.(THEOCHEM)* 901: 49.
- [41] Constantino, E., Rodríguez-Santiago, L., and Sodupe, M. 2005. *J. Phys. Chem. A.* 109: 224.
- [42] Koch, W., and Holthausen, M. C. 2001. *A Chemist's Guide to Density Functional Theory*. Germany: Wiley-VCH Verlag.
- [43] Jahromi, M. S., and Fattahi, A. 2009. *Chem. Chem. Eng.* 16: 75.
- [44] Raghab, P. 2012. *Acta Chim.Pharm. Indica.* 2: 85.
- [45] Meysam, N. 2014. *J. Mex. Chem. Soc.* 58: 36.
- [46] Balkabassis, E. G., Nemadis, E., and Tsimidou, M. 2003. *J. Am.Oil. Chem. Soc.* 80: 451.
- [47] Fiorucci, S., Golebiowski, J., Cabrol-Bass, D., and Antonczak, S. 2004. *Chem. Phys. Chem.* 5: 1726.
- [48] Fiorucci, S., Golebiowski, J., Cabrol-Bass, D., and Antonczak, S. 2007. *J. Agric. Food Chem.* 55: 903.